INTERNATIONAL JOURNAL FOR NUMERICAL AND ANALYTICAL METHODS IN GEOMECHANICS
*Int. J. Numer. Anal. Meth. Geomech.*, 2000; **24**:245–263

# Non-linear analysis of shear band formation in sand

Wei Wu*

*Lahmeyer International Ltd., 61118 Bad Vilbel, Germany*

## SUMMARY

The paper investigates the incipience of shear band with an incrementally non-linear constitutive equation. Necessary conditions for the emergence of shear band are derived. The lower bound solution is obtained by taking the strain rate inside and outside the shear band into consideration. Numerical results of localized bifurcation for general stress and strain are presented and compared with experiments. In the principal stress space, the stresses at the onset of shear band form a surface, which is partially enclosed by the failure surface for homogeneous straining. The significance of the analysis for identification of the material parameters and verification of the constitutive model against experiments is discussed. Copyright © 2000 John Wiley & Sons, Ltd.

KEY WORDS: shear band formation analysis; sand; granular materials; failure mechanism

## 1. INTRODUCTION

The significance of analysis of shear band formation is twofold. First, it may provide insight into the failure mechanism of granular materials. Second, it may serve as a touchstone for verifying constitutive models. However, as pointed out by Rice and Rudnicki[1] most of the analyses are performed using incrementally linear constitutive equations and concerned only with continuous localized bifurcation, where loading is assumed to occur both inside and outside the shear band. Recent experiments conducted by Tatsuoka *et al.*[2] indicate that the magnitude of strain rate outside the shear band can be comparable with that inside the shear band at the inception of shear band formation. Among the numerous theoretical investigations, an exception is due to Desrues and Chambon[3] with an incrementally non-linear model. Nevertheless, their constitutive model is of *ad hoc* nature and concerns only with plane strain tests.

Recently, there has been intensive research on incrementally non-linear models to reproduce the behaviour of granular materials.[4–12] The hypoplastic model underlying the shear band analysis is developed within the framework of rational mechanics and differs substantially from the elastoplastic models in that the key concepts in the plasticity theory, such as the yield surface, the flow rule and the decomposition of deformation into elastic and plastic parts are not needed.

The present paper follows the line of work by Wu and Sikora,[13] who showed that the analysis of localized bifurcation using hypoplastic constitutive equations results in a system of algebraic equations with an auxiliary condition. In a follow-up work,[14] numerical results are presented for

* Correspondence to: Dr.-Ing. W. Wu, Lahmeyer International Ltd., 61118 Bad Vilbel, Germany

*Received 17 June 1998*
*Revised 12 April 1999*

the case of plane strain. In the present paper, the previous work is generalized to the case of general stress and strain.

## 2. CONSTITUTIVE EQUATION

Let us consider the following hypoplastic constitutive equation proposed by Wu and Kolymbas:[15]

$$\mathring{\mathbf{T}} = \mathsf{L}(\mathbf{T}):\mathbf{D} + \mathbf{N}(\mathbf{T})\|\mathbf{D}\| \tag{1}$$

where $\mathbf{T}$ and $\mathbf{D}$ stand for the Cauchy stress tensor and the strain rate tensor, respectively. The Jaumann stress rate $\mathring{\mathbf{T}}$ is defined by

$$\mathring{\mathbf{T}} = \dot{\mathbf{T}} + \mathbf{T}\mathbf{W} - \mathbf{W}\mathbf{T} \tag{2}$$

where $\mathbf{W}$ denotes the spin tensor. The strain rate and spin tensors are related to the velocity gradient tensor through

$$\mathbf{D} = \tfrac{1}{2}(\partial\mathbf{v}/\partial\mathbf{x} + (\partial\mathbf{v}/\partial\mathbf{x})^{\mathrm{T}}) \tag{3}$$

$$\mathbf{W} = \tfrac{1}{2}(\partial\mathbf{v}/\partial\mathbf{x} - (\partial\mathbf{v}/\partial\mathbf{x})^{\mathrm{T}}) \tag{4}$$

$\mathsf{L}(\mathbf{T}):\mathbf{D}$ and $\mathbf{N}(\mathbf{T})$ in (1) are isotropic tensor-valued functions. $\mathsf{L}$ is a fourth-order tensor and the colon : denotes an inner product between two tensors, $\|\cdot\|$ stands for a norm and is defined by $\|\mathbf{D}\| = \sqrt{\mathbf{D}:\mathbf{D}}$. The following notation will be used throughout the paper: bold lower and upper case letters are used to denote vectors and tensors.

Granted that the behaviour to be described is rate independent, constitutive equation (1) is necessarily positively homogeneous of the first degree in $\mathbf{D}$. To show the difference between hypoplasticity and plasticity in more detail, constitutive equation (1) can be recast in a more convenient form by virtue of Euler's theorem for homogeneous functions

$$\mathring{\mathbf{T}} = (\mathsf{L} + \mathbf{N} \otimes \mathbf{D}):\mathbf{D} \tag{5}$$

where $\mathbf{D} = \mathbf{D}/\|\mathbf{D}\|$ stands for the direction of the strain rate: and the symbol $\otimes$ denotes as outer product between two tensors.

Constitutive equation (1) can be regarded pro forma as the sum of a linear part and a non-linear part. The two terms in the brackets in (5) represent the tangential stiffness tensor. It is apparent from (5) that the tangential stiffness tensor depends not only on stress but also on the direction of the strain rate. As compared with plasticity theory, hypoplastic constitutive models are incrementally non-linear. Note that the distinction between loading and unloading is of unimportance for the hypoplastic constitutive equation, since the non-linear part is always present irrespective of the direction of strain rate. Specific versions of constitutive equation (1) have been adopted to simulate various aspects of the mechanical behaviour of soils. In particular, the critical state has been included into the hypoplastic constitutive equation.[16]

## 3. FIELD EQUATIONS

Consider a homogeneous material element subjected to a uniform stress $\mathbf{T}$. For continued homogeneous deformation, the deformation velocity and velocity gradient fields are $\mathbf{v}$ and

 

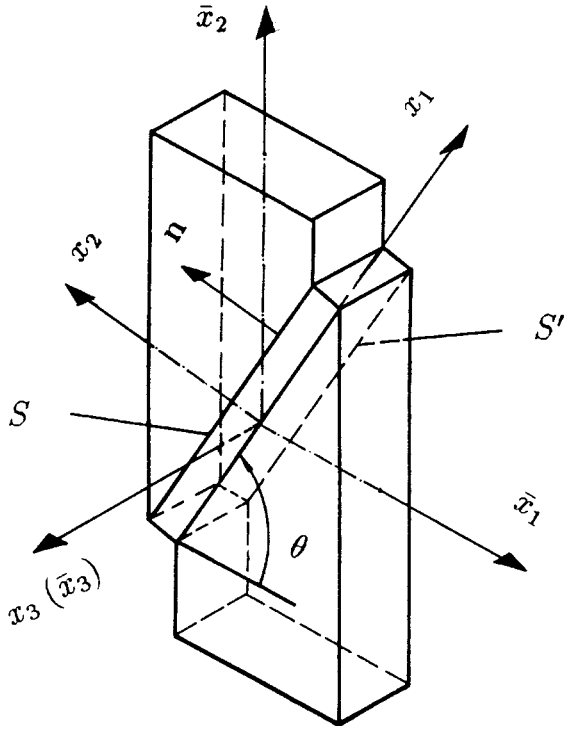


Figure 1. Co-ordinate system for the shear band

$(\partial \mathbf{v}/\partial \mathbf{x})$, respectively. We seek to determine whether the field equations admit, in addition to the homogeneous deformation, an alternative deformation field, where the velocity gradient exhibits a jump across a discontinuity surface. Figure 1 shows a shear band enclosed between two discontinuity surfaces $S$ and $S'$ and the corresponding local and global coordinate systems. With reference to Figure 1, the jump of the velocity gradient across the discontinuity surface, $S(\mathbf{x}) = 0$, can be written as follows:

$$[\![\partial \mathbf{v}/\partial \mathbf{x}]\!] = (\partial \mathbf{v}/\partial \mathbf{x})^{+} - (\partial \mathbf{v}/\partial \mathbf{x})^{-} \tag{6}$$

where the superscripts $+$ and $-$ refer to values of a field quantity directly in front of and behind the discontinuity surface and the brackets $[\![\cdot]\!]$ denote a jump of the bracketed quantity across the discontinuity surface. The shear band is assumed to be enclosed by a pair of regular surfaces, which separate the shear band from the neighbouring material. Assume further that the velocity itself is continuous in space. Making use of Hadamard's compatibility conditions for a discontinuous field of order one, it can be shown that the jump of the velocity gradient necessarily has the following dyadic structure:

$$[\![\partial \mathbf{v}/\partial \mathbf{x}]\!] = \mathbf{g} \otimes \mathbf{n} \tag{7}$$

in which $\mathbf{n} = (\partial S/\partial \mathbf{x})/\|\partial S/\partial \mathbf{x}\|$ is the unit vector normal to the discontinuity surface $S(\mathbf{x}) = 0$. Let us introduce the local coordinate system $\mathbf{x}$ such that $x_2$ is perpendicular to the discontinuity surface. In the local co-ordinate system $\mathbf{x}$, the jump of the velocity gradient possesses the

 

following simple expression:

$$[\![\partial \mathbf{v}/\partial \mathbf{x}]\!] = \begin{bmatrix} 0 & g_1 & 0 \\ 0 & g_2 & 0 \\ 0 & g_3 & 0 \end{bmatrix} \tag{8}$$

The strain rate and the spin tensors can be readily obtained via (3)

$$[\![\mathbf{D}]\!] = \tfrac{1}{2}(\mathbf{g} \otimes \mathbf{n} + \mathbf{n} \otimes \mathbf{g}) \tag{9}$$

$$[\![\mathbf{W}]\!] = \tfrac{1}{2}(\mathbf{g} \otimes \mathbf{n} - \mathbf{n} \otimes \mathbf{g}) \tag{10}$$

The stress and stress rate tensors in the co-ordinate systems $\mathbf{x}$ and $\bar{\mathbf{x}}$ are related by

$$\mathbf{T} = \mathbf{Q}\bar{\mathbf{T}}\mathbf{Q}^{\mathrm{T}}, \quad \dot{\mathbf{T}} = \mathbf{Q}\dot{\bar{\mathbf{T}}}\mathbf{Q}^{\mathrm{T}} \tag{11}$$

where $\mathbf{Q}$ is the transformation matrix from the local to the global coordinate system.[13]

At the inception of localized bifurcation, the stress is assumed to be in equilibrium. The continued equilibrium condition requires that

$$\operatorname{div} \dot{\mathbf{T}} = 0 \tag{12}$$

In view of (7), the stress rate is uniform outside the shear band and depend solely on $\mathbf{n} \cdot \bar{\mathbf{x}}$ inside the shear band. As a consequence, the traction must have the same value across the discontinuity surface. That is

$$[\![\dot{\mathbf{t}}]\!] = [\![\dot{\mathbf{T}}]\!]\mathbf{n} = \mathbf{0} \tag{13}$$

Before proceeding with the analysis of localized bifurcation, let us first consider the failure under homogeneous straining and define the corresponding failure criterion. A material element is at failure, if for a given $\mathbf{T}$ there exists a strain rate $\mathbf{D}$ such that

$$\mathring{\mathbf{T}} = \mathsf{L}(\mathbf{T}) : \mathbf{D} + \mathbf{N}(\mathbf{T})\|\mathbf{D}\| = 0 \tag{14}$$

If the set of stress satisfying the above equation forms a surface in the stress space, it will be called the failure surface. For details to determine the failure surface for hypoplastic constitutive equations, the reader is referred to the recent work by Wu and Niemunis.[10] In addition to the failure surface, a bound surface enclosing all accessible stress paths can be found for hypoplastic constitutive equations. For derivations of the bound surface we refer to Wu and Niemunis.[11]

A final remark is relevant to the restrictions placed on the jump of the stress rate by (13) and (14). Clearly, the failure condition for homogeneous straining (14) demands that all components of the stress rate tensor vanish at failure. Writing out (13) in the local co-ordinate system, we obtain the following equations restricting the jump of the stress rate at incipient bifurcation

$$[\![\dot{T}_{12}]\!] = [\![\dot{T}_{22}]\!] = [\![\dot{T}_{23}]\!] = 0 \tag{15}$$

In other words, only the rest three components of the stress rate tensor, i.e. $\dot{T}_{11}$, $\dot{T}_{13}$ and $\dot{T}_{33}$, may experience jumps at incipient bifurcation.

## 4. SHEAR BAND ANALYSIS

To facilitate numerical analysis, it is convenient to align the co-ordinates with the principal stress directions and write the tensors in constitutive equation (1) in matrix form. Assume that $\mathsf{L}(\mathbf{T})$ is

 

positively definite and that $\mathsf{L}(\mathbf{T}):\mathbf{D}$ is coaxial with $\mathbf{D}$. Note that the non-linear part $\mathbf{N}(\mathbf{T})\|\mathbf{D}\|$ is always coaxial with $\mathbf{T}$. The hypoplastic constitutive relation may be rewritten in the following matrix form:

$$\{\mathring{\mathbf{T}}\} = [\mathsf{L}]\{\mathbf{D}\} + \{\mathbf{N}\}\sqrt{\{\mathbf{D}\}^{\mathrm{T}}\{\mathbf{D}\}} \tag{16}$$

From the coaxiality of $\mathsf{L}(\mathbf{T}):\mathbf{D}$ with $\mathbf{D}$ and of $\mathbf{N}(\mathbf{T})\|\mathbf{D}\|$ with $\mathbf{T}$ follows that the strain rate $\mathbf{D}$ coaxial with the stress tensor $\mathbf{T}$ will result in coaxial stress rate. Note that the matrix $[\mathsf{L}]_{[9:9]}$ that maps the shear components of the strain rate $\{\mathbf{D}\}_{[9:1]}$ into the stress rate components is diagonal. In other words, considering the linear part in (16), there is no coupling between the normal components and the shear components, e.g. $D_{13}$ affects $\mathring{T}_{13}$ only. However, we will write the diagonal part of $\mathsf{L}(\mathbf{T})$ in a slightly different way. Instead of $T_{12} = 2L_{1212}\cdot D_{12}$, we use an equivalent expression $T_{12} = L_{1212}\cdot D_{12} + L_{1221}\cdot D_{21}$ where ${}_{ijkl} = L_{ijlk}$. This may be done since the stress rates and the stetching are symmetric tensors.

A further remark is concerned with the symmetry of the tangential stiffness tensor $\mathsf{L}(\mathbf{T})$. Because of symmetries in stress and strain rate we have always

$$L_{ijkl} = L_{ijlk} = L_{jikl} = L_{jilk} \tag{17}$$

Note that in general $L_{ijkl} \neq L_{klij}$ since the linear part, being hypoelastic, need not be derived from a potential. The symmetry $L_{ijkl} = L_{klij}$ can be shown iff the linear part is derivable from a potential.

Bearing in mind that the stress itself is continuous, the jump of the Jaumann stress rate can be obtained from (2)

$$[\![\mathring{\mathbf{T}}]\!] = [\![\dot{\mathbf{T}}]\!] + \mathbf{T}[\![\mathbf{W}]\!] - [\![\mathbf{W}]\!]\mathbf{T} \tag{18}$$

On the other hand, the jump of the stress rate can be obtained from constitutive equation (1)

$$[\![\mathring{\mathbf{T}}]\!] = \mathsf{L}(\mathbf{T}):[\![\mathbf{D}]\!] + \mathbf{N}(\|\mathbf{D}^{+}\| - \|\mathbf{D}^{-}\|) \tag{19}$$

Combining (18) and (19) yields the fundamental equation of localized bifurcation

$$(n_i L_{ijkl} n_l + A_{jk})g_k + n_i N_{ij}(\|\mathbf{D}^{+}\| - \|\mathbf{D}^{-}\|) = 0 \tag{20}$$

with

$$A_{jk} = n_i T_{ij} n_k - T_{kj} - n_j n_i T_{ik} + n_i T_{ir} n_r \delta_{jk} \tag{21}$$

in which $\delta_{ij}$ is the Kronecker symbol. In deriving (21) use has been made of the symmetry of $L_{ijkl}$ with respect to the indices $kl$. Analagous to the derivations in the propagation of acceleration waves, let us introduce the acoustic tensor $\bar{L}_{jk} = n_i L_{ijkl} n_l$. The acoustic tensor can be written out in the matrix form

$$[\bar{\mathbf{L}}] = \begin{bmatrix} \bar{L}_{11} & \bar{L}_{12} & \bar{L}_{13} \\ \bar{L}_{21} & \bar{L}_{22} & \bar{L}_{23} \\ \bar{L}_{31} & \bar{L}_{32} & \bar{L}_{33} \end{bmatrix} \tag{22}$$

 

where

$$\begin{aligned}
\bar{L}_{11} &= L_{1111}n_1^2 + L_{1212}n_2^2 + L_{1313}n_3^2 \\
\bar{L}_{12} &= (L_{1122} + L_{1212})n_1n_2 \\
\bar{L}_{13} &= (L_{1133} + L_{1313})n_1n_3 \\
\bar{L}_{21} &= (L_{2211} + L_{1212})n_2n_1 \\
\bar{L}_{22} &= (L_{2222}n_2^2 + L_{1212}n_1^2) + L_{2323}n_3^2 \\
\bar{L}_{23} &= (L_{2233} + L_{2323})n_2n_3 \\
\bar{L}_{31} &= (L_{3311} + L_{1313})n_3n_1 \\
\bar{L}_{32} &= (L_{3322} + L_{2323})n_3n_2 \\
\bar{L}_{33} &= (L_{3333}n_3^2 + L_{1313}n_1^2)L_{2323}n_2^2.
\end{aligned} \tag{23}$$

The tensor **A** can be written out in the following matrix form to give

$$[\mathbf{A}] = \begin{bmatrix} A_{11} & A_{12} & A_{13} \\ A_{21} & A_{22} & A_{23} \\ A_{31} & A_{32} & A_{33} \end{bmatrix} \tag{24}$$

where

$$\begin{aligned}
A_{11} &= \omega_i n_i - T_{11} \\
A_{12} &= \omega_1 n_2 - \omega_2 n_1 \\
A_{13} &= \omega_1 n_3 - \omega_3 n_1 \\
A_{21} &= \omega_2 n_1 - \omega_1 n_2 \\
A_{22} &= \omega_i n_i - T_{22} \\
A_{23} &= \omega_2 n_3 - \omega_3 n_2 \\
A_{31} &= \omega_3 n_1 - \omega_1 n_3 \\
A_{32} &= \omega_3 n_2 - \omega_2 n_3 \\
A_{33} &= \omega_i n_i - T_{33}.
\end{aligned} \tag{25}$$

where $\omega_i = T_{ij}n_j$ is obtained by summation over the mute index. Furthermore, let us introduce the vector $\bar{N}_i = N_{ij}n_j$ with the following matrix form:

$$\{\bar{\mathbf{N}}\} = \begin{Bmatrix} n_1N_{11} \\ n_2N_{22} \\ n_3N_{33} \end{Bmatrix} \tag{26}$$

With the above matrices for $[\bar{\mathbf{L}}]$, $[\mathbf{A}]$ and $[\bar{\mathbf{N}}]$, equation (20) can be cast in the matrix form convenient for the numerical solution

$$([\bar{\mathbf{L}}] + [\mathbf{A}])\{\mathbf{g}\} = -\{\bar{\mathbf{N}}\}(\|\mathbf{D}^+\| - \|\mathbf{D}^-\|) \tag{27}$$

 

It is interesting to observe that if the non-linear term $\mathbf{N}(\mathbf{T})$ is dropped, i.e. the hypoplastic constitutive equation degenerates to an incrementally linear constitutive equation, or equally if the magnitude-jump of the strain rate across the discontinuity surface vanishes, equation (27) reduces to a homogeneous equation system. The well-known bifurcation condition for incrementally linear constitutive equations is recovered.

To this end, the bifurcation analysis is equivalent to finding non-trivial solutions, i.e. $\mathbf{g} \neq 0$, of the above equation system. Note that equation (27) possesses a solution for a given magnitude jump ($\|\mathbf{D}^+\| - \|\mathbf{D}^-\|$) as long as the matrix ($[\bar{\mathbf{L}}] + [\mathbf{A}]$) is not singular. This remains so irrespective of the stress state (even for a hydrostatic stress state). Of course, this is contradictary to the experimental evidence.

To resolve the problem we need to have a closer look at the jump of strain rate across the shear band. We proceed to define the degree of bifurcation $d$ as follows:

$$d = \frac{\|[\![\mathbf{D}]\!]\|}{\|\mathbf{D}^+\| - \|\mathbf{D}^-\|} = \frac{\|\mathbf{D}^+ - \mathbf{D}^-\|}{\|\mathbf{D}^+\| - \|\mathbf{D}^-\|} \tag{28}$$

The geometrical meaning of $d$ is shown in Figure 2. It can be easily seen from Figure 2 that the jump of the strain rate tensor must fulfill the triangle inequality. This is equivalent to the requirement that the degree of bifurcation must be greater than or equal to unity.

$$d \geqslant 1 \tag{29}$$

Equation (27) together with the auxiliary equation (29) define the necessary condition of shear band formation for constitutive equation (1). Note that the solution of equation (27) is proportional to the magnitude jump of the strain rate ($\|\mathbf{D}^+\| - \|\mathbf{D}^-\|$). The stress level obtained from the solution of (27) is found to decrease with increasing ($\|\mathbf{D}^+\| - \|\mathbf{D}^-\|$). It is of interest to find the

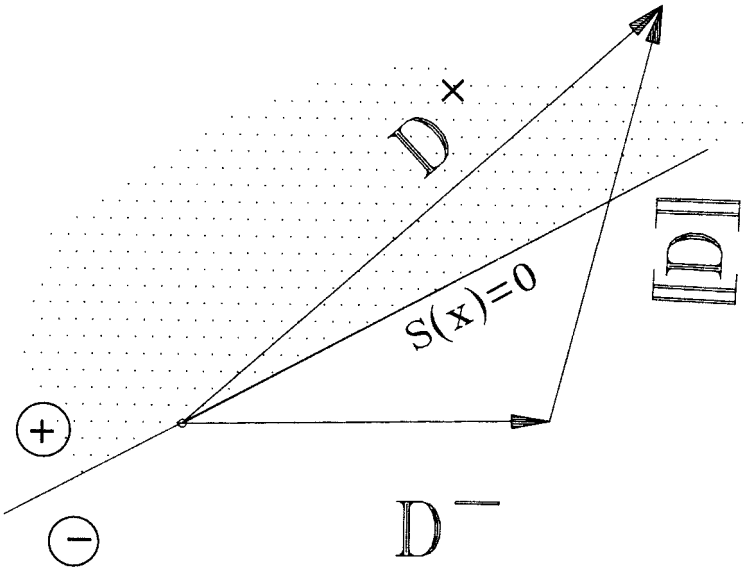


Figure 2. Geometrical meaning of the jump of the strain rate across $S(x)$

 

lowest stress level of bifurcation. On the other hand, the degree of bifurcation $d$, which is inversely proportional to $(\|\mathbf{D}^+\| - \|\mathbf{D}^-\|)$, must be greater than 1. It turns out that the lowest stress level of bifurcation is obtained at

$$d = \frac{\|\mathbf{D}^+ - \mathbf{D}^-\|}{\|\mathbf{D}^+\| - \|\mathbf{D}^-\|} = 1 \tag{30}$$

In this case, the solution of (27) provides the lower bound solution. If the set of stress forms a surface in the stress space, it will be called the bifurcation surface.

Note that the strain rates inside and outside the shear band, i.e. $\mathbf{D}^-$ and $\mathbf{D}^+$, are proportional or coaxial for the lower bound solution as can be assertained from (30). At first glance, this might sound strange, since the shear band formation is of localized nature with the deformation mode of the simple shear within the shear band. With a fully developed shear band in mind, the strain rates inside and outside the shear band are apparently not coaxial. However, this is only relevant to fully developed shear bands, while we are here concerned with the onset of shear band. In the present paper, the shear band formation is seen as an alternative to the homogeneous deformation. It is clear from (27) that the homogeneous deformation with $\mathbf{g} = \mathbf{0}$ is always met at the onset of shear banding. In fact, the shear band formation from the inception to the fully localized deformation mode can be viewed as a process. The onset of the process is marked by a deviation of the strain rate inside the shear band from outside in magnitude (the jump in magnitude). Upon further straining the jump in magnitude will grow accompanied by deviation in direction. As will be shown in the next section, the degree of bifurcation exceeds 1 beyond the bifurcation surface. Note further that the analysis provides only the necessary condition for shear banding. In other words, the shear band may occur beyond but not prior to the bifurcation surface. Note further that the analysis provides only the necessary condition for shear banding. In other words, the shear band may occur beyond but not prior to the bifurcation surface. It is worth noting that Loret[17] presented a shear band analysis with an incrementally non-linear model. Despite the *ad hoc* nature of his model, he arrived at the conclusion that the onset of shear banding depends on the strain rates on both sides of the shear band. Similar results were obtained by Petryk[18] based on a stress vertex model. However, his model is primarily applicable for metallic materials.

For an incrementally linear model, i.e. when the non-linear term in (27) vanishes, we are left with an eigenvalue problem. In this case, the solution does not provide any information on the strain rates inside and outside the shear band. In addition to the outcome in a linear analysis, e.g. the stress level and the inclination of shear band at the onset of shear banding, our analysis provides the additional information on the strain rates inside and outside the shear band. An ensuing question is how the strain rate manifests itself in the laboratory test. For this purpose, the results of a plane strain test on dense Toyoura sand is shown in Figures 3 and 4.[2] Figure 4 shows the distribution of the strain rate measured at different axial strain (stress level) of the stress–strain curve in Figure 3. Before the peak on the stress–strain curve, the strain rate is homogeneous as can be seen from Figure 4(a) and 4(b). Figure 4(c) shows the strain rate distribution immediately after the peak and marks the onset of shear band. At this time instant there is only minor difference between the strain rate inside and outside the shear band. The deviation becomes more pronounced with increasing axial strain from Figure 4(c) to 4(f) accompanied by a strong strain softening on the stress–strain curve. Figure 4(f) shows a nearly rigid deformation mode outside the shear band. The deformation becomes localized in the shear band, which is typical for a fully developed shear band. The experimental results seem to support our analysis in that there is no striking jump of the strain rate at the onset of shear banding.

 

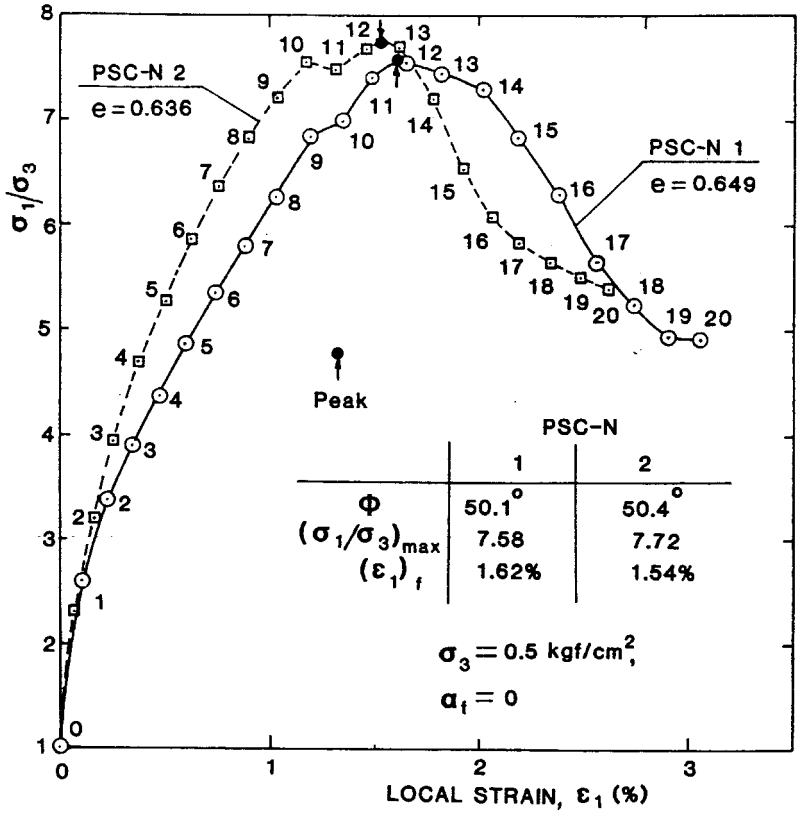


Figure 3. Stress–strain curve of a plane strain test on dense Toyoura sand after Tatsuoka *et al.*[2] (courtesy of Prof. Tatsuoka of Tokyo University)

At this stage, it is interesting to recall the shear band analysis by Kolymbas,[19] where the strain rate outside the shear band is assumed to vanish, i.e. the sand specimen outside the shear band behaves like a rigid body. This assumption of rigid deformation mode turns out to be a special case of (27) with (30) trivially fulfilled. While the rigid deformation mode is realistic for a fully developed shear band as can be seen from Figure 4(f), it is certainly not appropriate at the inception of shear band.

On the bifurcation surface the shear band emerges only for one particular direction of strain rate, i.e. $\mathbf{D}^- \propto \mathbf{D}^+ \propto [\![\mathbf{D}]\!] = \frac{1}{2}(\mathbf{n} \otimes \mathbf{g} + \mathbf{g} \otimes \mathbf{n})$. Consider the problem of bifurcation in a process of monotonic loading, e.g. in a triaxial compression test. The strain rate $\mathbf{D}^-$ results from the constitutive relation and is usually not proportional to the jump $[\![\mathbf{D}]\!]$ required by the condition of bifurcation. In such a case the bifurcation may be delayed. As will be shown in the next section, the onset of shear band in triaxial compression is met after the failure under homogeneous straining.

A final remark is concerned with the fact that our analysis deals only with the onset of shear band. The analysis after the onset of shear band will inevitably involve the thickness of the shear band and the material behaviour inside and outside the shear band[20] which is beyond the scope of the present paper.

 

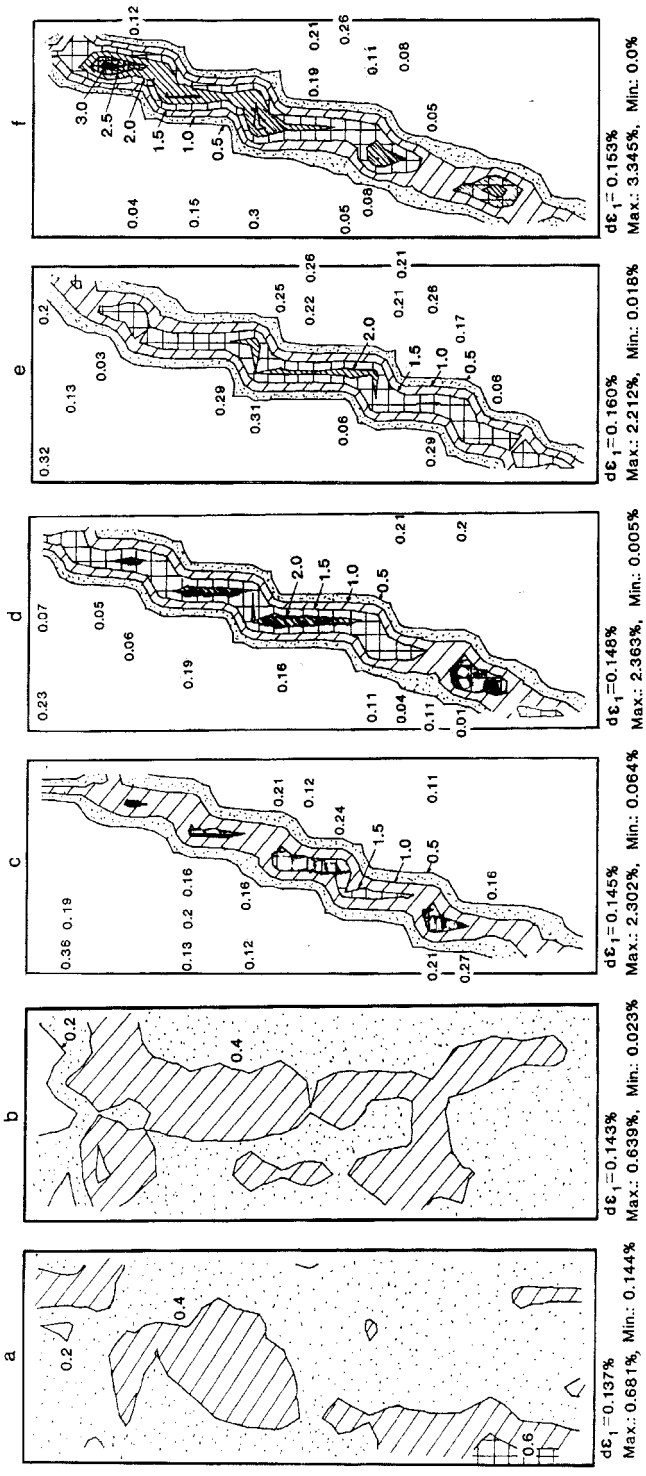


Figure 4. Strain rate distribution at different stress level of the stress–strain curve PSC-N 2 in Figure 3 (through numbers marked on the curve): The measurements were made between (a) 8 and 9 (b) 9 and 10 (c) 10 and 11 (d) 11 and 12 (e) 12 and 13 (f) 13 and 14

## 5. NUMERICAL RESULTS

In order to obtain numerical results we turn our attention to the following specific version of hypoplastic constitutive equation proposed by Wu[21]

$$\mathring{\mathbf{T}} = C_1(\mathrm{tr}\,\mathbf{T})\mathbf{D} + C_2\frac{(\mathbf{T}:\mathbf{D})\mathbf{T}}{\mathrm{tr}\,\mathbf{T}} + \left(C_3\frac{\mathbf{T}^2}{\mathrm{tr}\,\mathbf{T}} + C_4\frac{\mathbf{T}^{*2}}{\mathrm{tr}\,\mathbf{T}}\right)\|\mathbf{D}\| \tag{31}$$

where $C_i (i = 1, \ldots, 4)$ are dimensionless constants. The deviatoric stress tensor in equation (31) is defined by $\mathbf{T}^* = \mathbf{T} - \frac{1}{3}(\mathrm{tr}\,\mathbf{T})\mathbf{1}$. For the performance of the above constitutive equation we refer to the work by Wu and Bauer.[7] The following material constants, typical for dense sand, are used for the numerical calculation: $C = -106{\cdot}5$, $C_2 = -801{\cdot}5$, $C_3 = -791{\cdot}1$, $C_4 = 1077{\cdot}7$.

Figure 5 shows the numerical result of a plane strain test. Figure 5(a) shows the stress–strain curve under homogeneous deformation. The stress–strain curve reaches a horizontal asymptote, which characterizes the shear strength under homogeneous deformation. As can be seen from Figure 5(b), we have, starting from the hydrostatic stress, initially $d < 1$. Along with the deformation the degree of bifurcation increases until $d = 1$ is met. Point A marks the lower bound solution. The lower bound solution is seen to be unique. Beyond point A the degree of bifurcation increases slightly and then assumes a constant value. Figure 5(c) shows that the inclination of shear band is about 60° at $d = 1$ and lies between 50 and 70° for $d > 1$.

Next, the bifurcation surface in the stress space is considered. We confine our attention to a deviatoric stress plane with $\mathrm{tr}\,\mathbf{T} = -1$. To facilitate numerical solution, the three principal stresses are expressed by the three invariants, $r$, $\psi$ and $\mathrm{tr}\,\mathbf{T}$, of the stress tensor

$$\mathrm{T}_i = \sqrt{\frac{2}{3}}\,r\sin\left(\psi + \frac{2\pi(2-\mathrm{i})}{3}\right) + \mathrm{tr}\,\mathbf{T} \tag{32}$$

where

$$r = \frac{1}{\sqrt{3}}\sqrt{(\mathrm{T}_1 - \mathrm{T}_2)^2 + (\mathrm{T}_2 - \mathrm{T}_3)^2 + (\mathrm{T}_3 - \mathrm{T}_1)^2} \tag{33}$$

$$\psi = \arctan\frac{1}{\sqrt{3}}\,\frac{2\mathrm{T}_2 - \mathrm{T}_1 - \mathrm{T}_3}{\mathrm{T}_1 - \mathrm{T}_3} \tag{34}$$

$r$ is the radius of the stress vector on the deviatoric plane and $\psi$ is the so-called Lode angle.

In solving equations (27) and (30) the Lode angle $\psi$ is varied from 0 to $2\pi$. For each $\psi$ the radius $r$ is increased from zero, corresponding to a hydrostatic stress state, until the equations are fulfilled. In the present paper, equations (27) and (30) are solved with the regula-falsi method. On solving equations (27) and (30), the following dilatancy angle can be calculated

$$v = \arctan\frac{g_2}{g_1} \tag{35}$$

$v$ characterises the dilatancy within the shear band at incipient bifurcation.

The numerical results obtained with the constitutive equation (31) are shown in Figure 6. It can be see from Figure 6(a) that the stress states of possible localized bifurcation form a surface in the stress space. Figure 6(a) shows that localized bifurcation generally occurs prior to homogeneous failure and is not restricted to the cases of plane strain. An interesting feature of Figure 6(a) is that

 

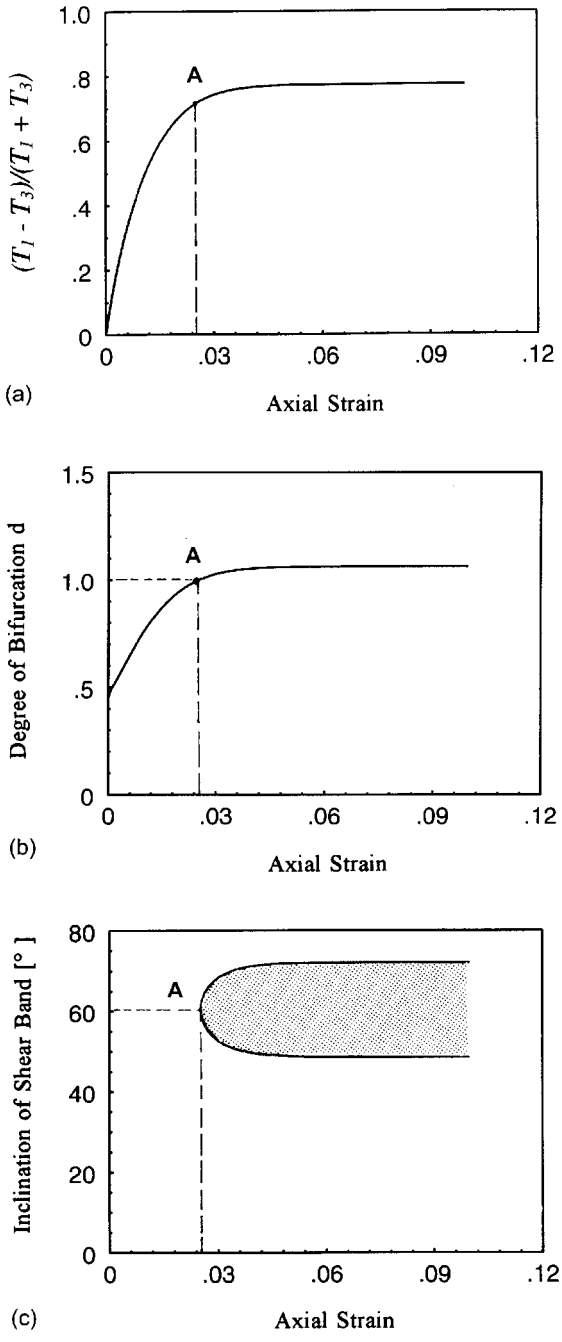


Figure 5. Numerical simulation of a plane strain test with an isotropic consolidation stress of 100 kPa

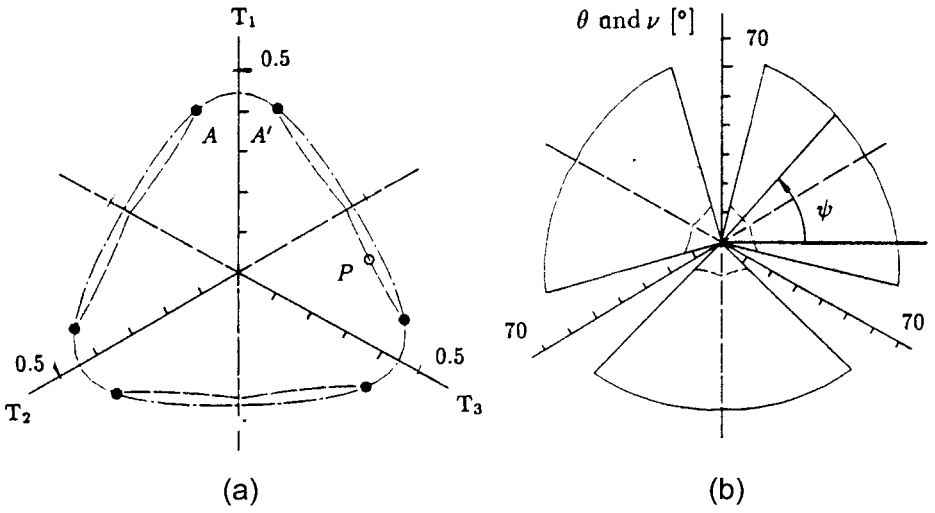


Figure 6. Numerical results of the bifurcation surface: (a) the failure and localization surface calculated on an octahedral stress plane: (—·—) failure surface, (– – –) bifurcation surface; (b) variation of the shear band inclination and of the dilatancy angle with the Lode angle $\psi$: (——) orientation of the shear band. (— — —) dilatancy angle

in the vicinity of compressive axisymmetric loading localization merges with homogeneous failure at points $A$ and $A'$, whereas for plane strain loading (point $P$ in Figure 5(a)) localization is met much earlier homogeneous failure. This is in agreement with the experimental observation that the specimen in a plane strain test is prone to shear band formation, whereas no localization occurs in a compressive axisymmetric test before homogeneous failure. Rudnicki and Rice[22] arrived at the same conclusion using an elastic–plastic constitutive equation. Nevertheless, unlike the three-dimensional analysis in the present paper they treated only the problem of axisymmetry and of plane strain. The dilatancy angle in Figure 6(b) varies with the Lode angle in a similar manner as the bifurcation surface in Figure 6(a). The orientation of the shear band in Figure 6(b) changes only slightly with the Lode angle. In Figure 7 the bifurcation, failure and bound surfaces are depicted in the three-dimensional principal stress space.

That the degree of bifurcation is greater than unity outside the bifurcation surface and less than unity inside, is demonstrated in Figure 8 by presenting $d$ against the two angles of the vector $\mathbf{n}$ in the spherical co-ordinate system. Figures 8(a) and 6(b) are obtained for a stress state outside and inside the bifurcation surface, respectively. The cut-off is set at $d = 1$. While $d$ is seen to be greater than unity for the stress outside the bifurcation surface (Figure 8(a)), $d$ is less than unity in all directions for the stress inside the bifurcation surface (Figure 8(b)). The four peaks indicate that there are two complementary orthogonal shear bands.

## 6. COMPARISON WITH EXPERIMENTS

The significance of the above analysis is twofold. The first aspect is concerned with identification of the material parameters in the constitutive model while the second aspect is related to comparison of the predictions of the constitutive model with experiments.

 

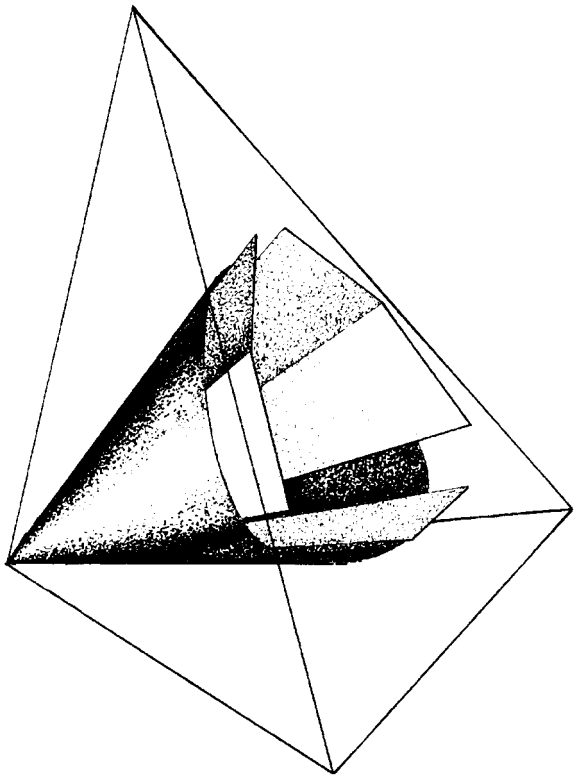

Figure 7. Visualization of the failure surface and the bifurcation surface in the principal stress space

Since the constitutive models are developed with reference to a material element subjected to uniform stress and strain, only those experiments with uniform stress and strain are suited for identification of the parameters in the constitutive model. Experiments with granular materials, such as dry sand, show that shear banding occurs prior to homogeneous failure for plane strain tests.[2,23] For triaxial compression tests, however, homogeneous failure is observed before shear banding.[5,24] This suggests that the constitutive model should be calibrated with reference to triaxial compression tests rather than plain strain tests.

There exists a large amount of experimental data of the stress at failure obtained in triaxial apparatus with independent control of the three principal stresses.[25,26] Many investigators attempt to fit the experimental data with failure surfaces. This is not appropriate, since the experimental data involve shear banding, while the failure surface in the constitutive model is assumed for homogeneous straining. In Figure 9 the experimental data on dense Karlsruhe sand are shown together with the failure and bifurcation surface on a deviatoric plane. The triaxial apparatus is of strain control. We believe that the agreement between the bifurcation surface and the test data is not a coincidence but an indication of shear band formation. It is interesting to observe that the data near triaxial compression (full points) comply well with the failure surface. We suppose that the homogeneous failure dominates in the vicinity of triaxial compression.

 

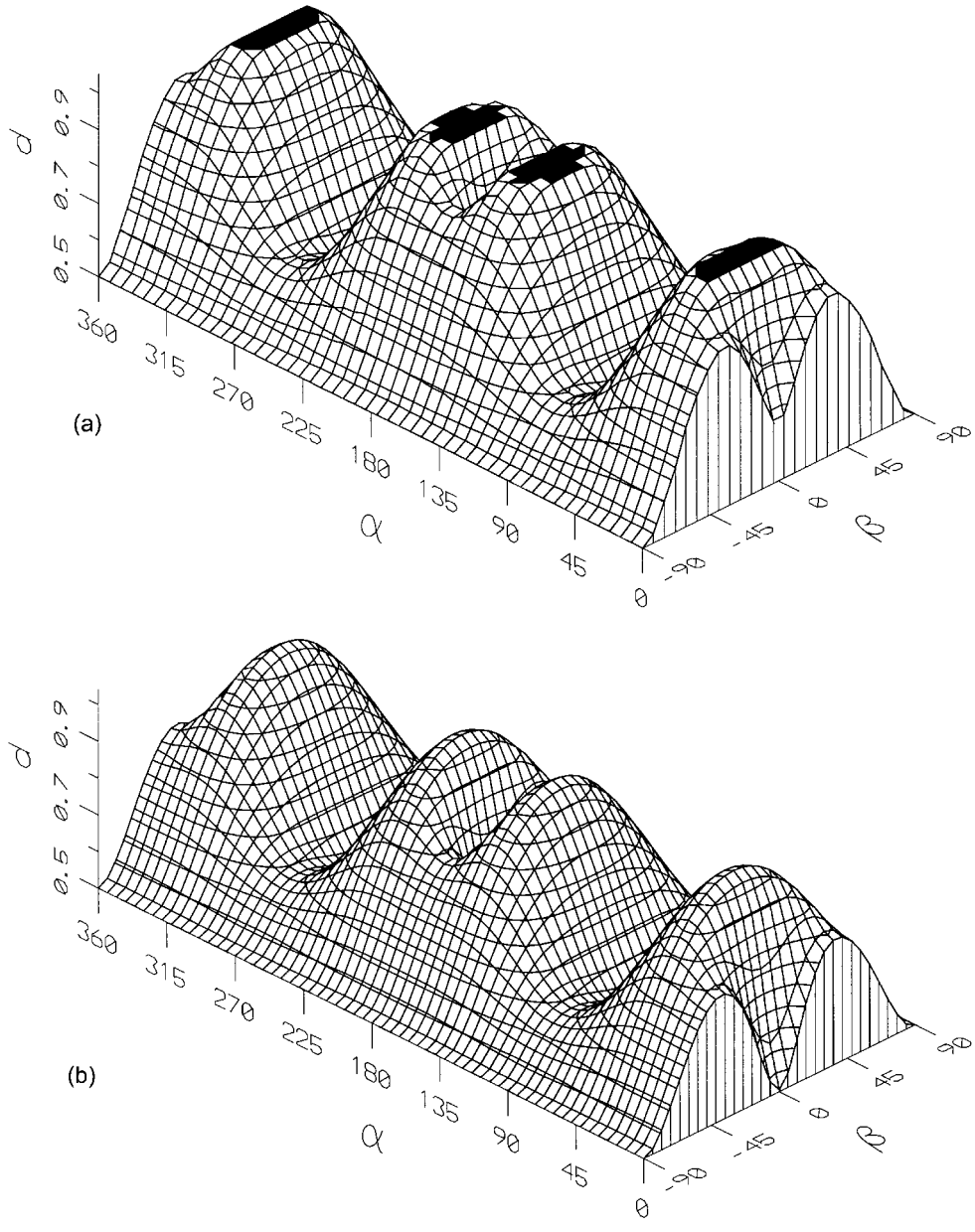


Figure 8. Evolution of the degree of bifurcation: (a) for a stress state outside the bifurcation surface; (b) for a stress state inside the bifurcation surface

It is not always possible to have visual observation of the incipience of shear band, since the specimen is enclosed in a rubber bag. An alternative is to judge from the measured stress–strain curve, since shear banding is frequently accompanied by pronounced strain softening,[27] The

 

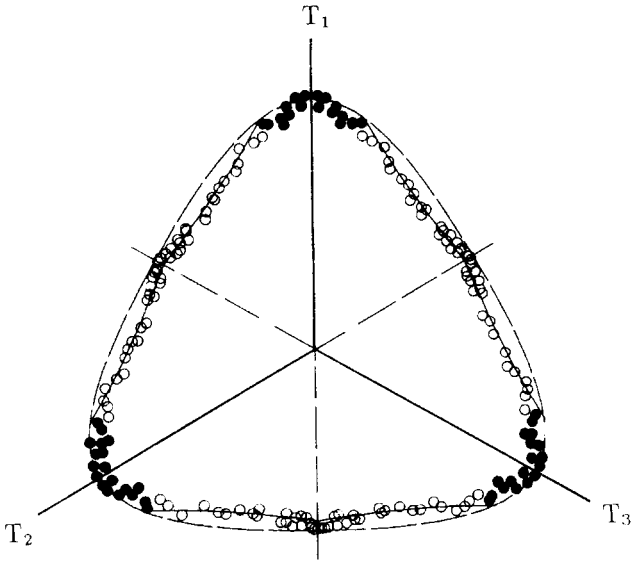


Figure 9. Comparison with tests on dense sand by Goldscheider[26]

above analysis shows that homogeneous failure is only possible for stress paths lying in a small sector around triaxial compression. Experimental results with dense Ham river sand carried out in a triaxial apparatus with independent stress control by Reades and Green[25] are shown in Figure 10. Strong strain softening is observed everywhere except near triaxial compression. Our analysis is well corroborated by this experimental finding.

## 7. CONCLUSION

An analysis of shear band formation with an incrementally non-linear constitutive model is presented. The outcome of the analysis is interesting on several accounts. First, the constitutive model is not tailored for the shear band analysis. In this sense, the results are not reproduction of known facts but predictions, see e.g. Figure 9. Second, the case of general stress and strain is considered. As a consequence, the results are valid for all boundary conditions, as is the case in various kinds of laboratory test. Finally, unlike the incrementally linear models, the strain rate outside the shear band is taken into consideration in our analysis. This feature is particularly appealing, when a rate-dependent model is concerned. A rate-dependent model within the framework of hypoplasticity has been proposed by Wu *et al.*[28] The shear band analysis with the rate-dependent model is ongoing and the results will be presented in a forthcoming publication. Another interesting aspect of shear band analysis concerns the problem of inherent anisotropy. As a matter of fact, all geomaterials show anisotropy to some extent. The impact of anisotropy on the shear band formation has been scarcely treated in the past. The recent work by Wu[12] presents a simple yet effective way to account for inherent anisotropy. It will be interesting to extend the analysis to account for the effect of inherent anisotropy.

 

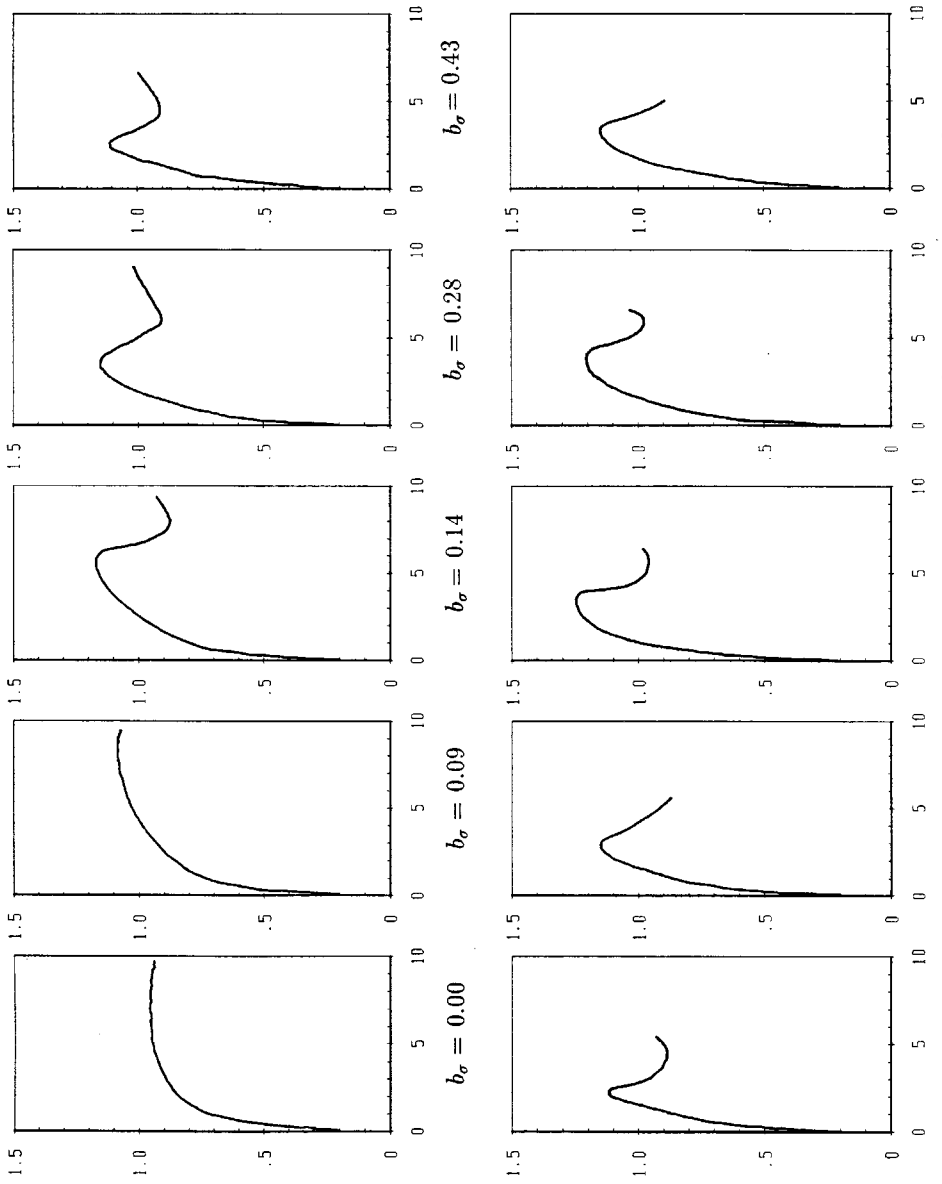


Figure 10. Major principal stress in [MPa] versus major principal strain in [after Reades and Green.[23]]. The stress parameter is defined by $b_\sigma = (T_2 - T_3)/(T_1 - T_3)$

ACKNOWLEDGEMENTS

The author is grateful to Dr. Niemunis at the Institute of Soil Mechanics and Foundation Engineering, Bochuum University, Germany for discussions when preparing the paper.

## REFERENCES

1. J. R. Rice and J. W. Rudnicki, 'A note on some features of the theory of localization of deformation', *Int. J. Solids Struct*., **16,** 597–605 (1980).
2. F. Tatsuoka, S. Nakamura, C. Huang and K. Tani, 'Strength anisotropy and shear band direction in plane strain tests of sand', *Soils Foundations*, **10,** 3554 (1990).
3. J. Desrues and R. Chambon, 'Shear band analysis for granular materials: the question of incremental non-linearity, *Ingenieur-Archiv*, **59,** 187–196 (1989).
4. D. Kolymbas, 'Eine konstruktive Theorie für Böden und andere körnige Stoffe', *Dissertation*, Karlsruhe University, Germany, 1988.
5. W. Wu and D. Kolymbas, 'On some issues in triaxial extension tests', *ASTM Geotech. Testing J*., **14,** 276–287 (1991).
6. F. Darve, 'The expression of rheological laws in incremental form and the main classes of constitutive equations', in F. Darve (ed), *Geomaterials*: *Constitutive Equations and Modelling*, Elsevier Applied Science, Amsterdam, 1990, pp. 123–147.
7. W. Wu and E. Bauer, 'A simple hypoplastic constitutive model for sand', *Int. J. Numer. Anal. Meth. Geomech*., **18,** 833–862 (1994).
8. R. Chambon, J. Desrues, W. Hammad and R. Charlier, 'CLoE, a new rate-type constitutive model for geomaterials, theoretical basis and implementation', *Int. J. Numer. Anal. Meth. Geomech.* **18,** 253–278 (1994).
9. D. Kolymbas, I. Herle and A. Wolffersdorff, 'Hypoplastic constitutive equation with internal state variables', *Int. J. Numer. Anal. Meth. Geomech*., **19,** 415–436 (1995).
10. W. Wu and A. Niemunis, 'Failure criterion, flow rule and dissipation function derived from hypoplasticity', *Mech. Cohesive-Frictional Mater*., **1,** 145–163 (1996).
11. W. Wu and A. Niemunis, 'Beyond failure in granular materials', *Int. J. Numer. Anal. Meth. Geomech*., **21,** 153–174 (1997).
12. W. Wu, 'Rational approach to anisotropy of sand', *Int. J. Numer. Anal. Meth. Geomech*., **22,** 921–940 (1998).
13. W. Wu and Z. Sikora, 'Localized bifurcation in hypoplasticity', *Int. J. Engng. Sci*., **29,** 195–201 (1991).
14. Z. Sikora and W. Wu, 'Shear band formation in biaxial tests', *Proc. Int. Conf. Constitutive Laws for Engineering Materials*, Elsevier Amsterdam, 1991, pp. 111–116.
15. W. Wu and D. Kolymbas, 'Numerical testing of the stability criterion for hypoplastic constitutive equations', *Mech. Mater*., **9,** 245–253 (1990).
16. W. Wu, E. Bauer and D. Kolymbas, 'Hypoplastic constitutive model with critical state for granular materials', *Mech. Mater*., **23,** 45–69 (1996).
17. B. Loret, 'Non-linéarité incrémentale et localisation des déformation: quelques remarque', *J. Theor. Appl. Mech*., **6,** 423–459 (1987).
18. H. Petryk, 'Material instability and strain-rate discontinuities in incrementally nonlinear continua', *J. Mech. Phys. Solids*, **40,** 1227–1250 (1992).
19. D. Kolymbas, 'Bifurcation analysis for sand sample with nonlinear constitutive equations', *Ing. Arch.* **50,** 131–140 (1981).
20. B. Mühlhaus and I. Vardoulakis, 'The thickness of shear bands in granular materials', *Géotechnique*, **37,** 271–283 (1987).
21. W. Wu, 'Hypoplastizität als mathematisches Modell zum mechanischen Verhalten granularer Stoffe', *Dissertation*, Karlsruhe University, Germany, 1992.
22. J. W. Rudnicki and J. R. Rice, 'Conditions for the localization of deformation in pressure sensitive dilatant materials', *J. Mech. Phys. Solids*, **23,** 371–394 (1975).
23. I. Vardoulakis, 'Shear band inclination and shear modulus of sand in biaxial tests', *Int. J. Numer. Anal. Meth. Geomech*., **2,** 103–119 (1980).
24. P. Lade, 'Localization effects in triaxial tests on sand', *Proc. IUTAM Conf. on Deformation and Failure of Granular Materials*, Balkema, Rotterdam, 1982, pp. 461–471.
25. D. Reades and G. E. Green, 'Independent stress control and triaxial extension tests on sand', *Géotechnique*, **26,** 551–576 (1976).
26. M. Goldscheider, 'Grenzbedingung und Fileßregel von Sand', *Mech. Res. Comm*., **3,** 463–468 (1976).

 

27. A. Drescher and I. Vardoulakis, 'Geometric softening in triaxial tests on granular material, *Géotechnique*, **32,** 291–303 (1982).
28. W. Wu, E. Bauer, A. Niemunis and I. Herle, 'Visco-hypoplastic models for cohesive soils', in D. Kolymbas (ed.), *Proc. Modern Approaches to Plasticity*, Elsevier, Amsterdam, pp. 365–383.

 